JOURNAL OF OPTOELECTRONICS AND ADVANCED MATERIALS Vol. 12, No. 4, April 2010, p. 868 - 871

Influence of Co on transport properties of $La_{0.54}Ho_{0.11}Sr_{0.35}Co_xMn_{1-x}O_3$ manganites

M.-L. CRAUS[a,b] M. LOZOVAN[a], N. CORNEI[c], V. SIMKIN[b]
[a]*National Institute of Research and Development for Technical Physics, Blvd D. Mangeron 47, Iasi, 700050, Romania*
[b]*Joint Institute for Nuclear Research, Joliot Curie 6, Dubna 141980, Mosk.Region, Russia*
[c]*"Al.I.Cuza" University", Chemistry Faculty, Carol I 11, 700506 Iasi, Romania*

The paper investigate how the structural and magnetic properties and magnetoresistance of the $La_{0.54}Ho_{0.11}Sr_{0.35}Mn_{1-x}Co_xO_3$ change with the increase of Co content. Manganites were prepared using a conventional solid-state ceramic route. The phase composition of the samples was monitorized by XRD, at room temperature, data being handled with CellRef and suitable Rietveld programs. All synthesized compounds contain as major phase a manganite (Pbnm (SG 62)). The magnetic and transport properties of the samples were performed by means of a Foner-type magnetometer and four probe method, at 1 T, respectively, H_{max}=2 T, between 77 and 400 K.

(Received April 7, 2010; accepted April 26, 2010)

Keywords: Manganites, Transport phenomena, Magnetic structure

1. Introduction

The perovskite manganites $Re_{1-x}Alk_x(M,T)O_3$ (covering a wide range of materials where Re is a trivalent rare-earth ion, Alk=Ca, Sr, Ba and T= Cr, Cu, Fe, Ni, Ti and Zn) were extensively studied in the last years due to magnetoresistive property near room temperature and their scientific and technological application [1-3]. The substitutions lead to a reduction of Curie temperature (T_C) and magnetization (σ, p), an increase of resistivity, and an enhancement of the magnetoresistance. On the other hand some $ACoO_3$ oxides exhibit also magnetoresistance properties which depend on the A and B-site elements and their ratio [4, 5]. Two CMR effects characterise the magnetoresistive manganites: intrinsic CMR and extrinsic CMR. For most CMR manganites the maximum CMR is obtained near the metal-insulator (MI) transition temperature T_{MI}, accompanied by a simultaneous ferromagnetic-paramagnetic (FM–PM) transition at the Curie temperature. This is so-called intrinsic CMR [6]. The intrinsic CMR effect, caused by the double exchange (DE) mechanism proposed by Zener, can explain the CMR phenomenon mostly observed near T_C [7]. However, the extrinsic CMR, which appears at the temperature $T < T_C$, is related to natural and artificial grain boundaries [8, 9] and is the important source of low-field magnetoresistance in polycrystalline samples.

The physical properties of the perovskite manganites are determined by the Mn 3*d* electrons. The Mn ions are coordinated in MnO_6 octahedra. The nearly cubic crystal field splits the 3d levels into an e_g doublet and a t_{2g} triplet at lower energy. Hole doping results in a mixed valence state of $(1-x)Mn^{3+}$, d^4, and (x) Mn^{4+}, d^3, ions. The CMR effect is supposed to arise from the competition of the coupling to local JT distortions and the kinetic energy of e_g electrons [10]. The spin-orbital model considers existence the e_g and t_{2g} superexchange (SE) between adjacent Mn^{3+} ions in the strong-coupling limit. The DE/SE interactions ratio depends on the geometrical features of the perovskite structure. If Mn cations are partially substituted by Co ions, the DE interaction between Mn^{3+} and Mn^{4+} could be destroyed to some extend. The crystal-field splitting of Co d states and Hund's rule exchange energy are comparable in magnitude, so that the energy gap between t_{2g} and e_g levels is rather small, which leads to intermediate and/or high spin states of $Co^{2+/3+}$ ions at higher temperatures ($T > 200$ K) [11].

In present paper, we reported results concerning transport phenomena and magnetic structure of $La_{0.54}Ho_{0.11}Sr_{0...35}Co_xMn_{1-x}O_3$ (LHSCMO) perovskites.

2. Experimental

The samples, $La_{0.54}Ho_{0.11}Sr_{0.35}Co_xMn_{1-x}O_3$ (LHSCMO) with the chemical composition with x= 0.05, 0.10, 0.15 and 0.20, were synthesized by ceramic method, using as precursors rare earth oxides (La_2O_3, Ho_2O_3), $SrCO_3$, $Co(NO_3)_2).6H_2O$ and $Mn(CH_3COO)_2{\cdot}4H_2O$. We performed also a test to obtain a cobaltite with the $La_{0.54}Ho_{0.11}Sr_{0.35}CoO_3$ chemical nominal composition. The precursors were mixed in corresponding stoichiometric ratios and calcinated at 400°C to decompose the organic constituents. The resulted powders were ground and pressed into pellets and presintered at 800°C for 17 hours in air. The presintered samples were again ground and finally sintered at 1200°C for 12 hours in air atmosphere.

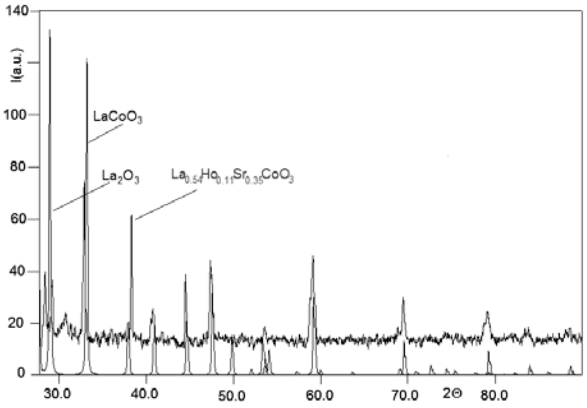

Fig. 1 Identification of cobaltite and lanthanum oxide similar phases in $La_{0.54}Ho_{0.11}Sr_{0.35}CoO_3$ sample (nominal composition).

Phase composition, structure, lattice constants, volume of the unit cell, distances between atoms and the Mn-O-Mn bond angles were determined by X-ray analysis using a diffractometer, equipped with a Cu X-ray tube and previewed with a data acquisition system, working at room temperature. The XRD data were handled with DICVOL/CheckCell/Powder programs. The best fit was obtained for an orthorhombic structure, Pbnm (GS 62), with La, Ho and Sr on (4c) site (x; y; 0.25), Mn on (4b) site (0.5; 0.0; 0.0), O_{ap} on (4c) site (apical positions; x1; y1; 0.25) and O_{eq} 0n (8d) site (equatorial positions; x2; y2; z2). x, x1, y and z2 are close on zero, y1 on ½, and x2 and y2 on ¼.

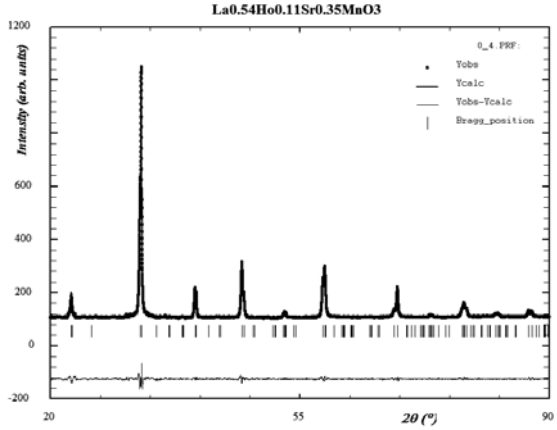

Fig. 2. Observed (black), calculated (red) and difference between the observed and calculated diffractograms for $La_{0.54}Ho_{0.11}Sr_{0.35}MnO_3$ (parent compound of the investigated samples). Bragg maximum positions are marked with green (Fullprof method).

The foreign phases, present in small amounts (except $La_{0.54}Ho_{0.11}Sr_{0.35}CoO_3$ cobaltite, x=1.0), were identified with the corresponding data from literature (s. Fig.1). This sample contains a typical cobaltite, as major phase, and an important amount of a similar as structure La_2O_3 phase (s. Fig.1). Because the diffractogram corresponding to $LaCoO_3$ and La_2O_3 did not superpose exactly on the maxima corresponding to the $La_{0.54}Ho_{0.11}Sr_{0.35}CoO_3$ sample we consider that the chemical compositions of identified phases are different from those of pure cobaltite ($LaCoO_3$) and lanthanum oxide, respectively. The space groups for the samples corresponding to x=0.05, 0.10, 0.15 and 0.20 were selected by means of the CeckCell program. The lattice constants, positions of cations and anions in the unit cell, distances Mn(Co)-O and B-O-B angles (in ABO_3 perovskite) were determined by using a Rietveld code (s. Fig.2). The magnetic and transport measurements were performed between 77 and 350 K by using a Foner-type magnetometer and, respectively, by means of four probe method.

3. Results and discussion

XRD patterns indicated that all samples investigated samples, except those corresponding to x=1.0, contain an orthorhombic (Pbnm) majority phases (> 98%). The unit-cell volumes (V) and average size of the coherent blocks (D) with Co concentration are plotted in Fig. 3. The decrease of unit-cell volume, for the samples with x < 0.15, suggested that this decrease is not only related to the difference in ionic radii between Mn (2)$r_{Mn3+(LS)}$= 0.72Å, $r_{Mn3+(HS)}$= 0.785Å, r_{Mn4+}= 0.58 Å) and Co ($r_{Co2+(LS)}$= 0.79Å, $r_{Co2+(HS)}$= 0.885Å, $r_{Co3+(LS)}$= 0.685Å, $r_{Co3+(HS)}$= 0.785Å) ions, but also due to the increase of the degree of covalent character in bonds (s. Tab.2, d_{MnOeq}) between the transition metal atom and the surrounding oxygen atoms.

Table 1. Lattice constants (a, b, c) and unit cell volume (V) for LHSCMO manganites.

x	a (Å)	b (Å)	c (Å)	V ($Å^3$)
0.05	5.4578	5.4754	7.6893	229.784
0.10	5.4502	5.4841	7.6872	229.766
0.15	5.4498	5.4875	7.6925	230.050
0.20	5.4598	5.4974	7.6950	231.457

Table 2. Mn-O_{ap} (d_{MnOap}), Mn-O_{eq} (d_{MnOeq}) distances, Mn-O_{ap}-Mn, (∠Mn-O_{ap}-Mn) and Mn-O_{eq}-Mn (∠Mn-O_{eq}-Mn) angles for LHSCMO manganites.

x	d_{MnOap} (Å)	∠Mn-O_{ap}-Mn (^{o})	d_{MnOeq} (Å)	∠Mn-O_{eq}-Mn (^{o})
0.05	1.9502	160.785	1.9596	161.550
0.10	1.9492	160.771	1.9576	161.547
0.15	1.9582	160.803	1.9523	161.525
0.20	1.9648	160.968	1.9576	161.408

An increase of the microstrains with the increase of the Co concentration was also observed. We explained this

behaviour by the increase of the local distortions on the Jahn-Teller effect that it depends on both Mn^{3+}/Mn^{4+} and Co^{2+}/Co^{3+} concentrations or/and on the presence of the foreign phase in the samples.

The Curie temperature was determined in agreement with the magnetic methods used in the study of manganites. From the variation of the molar magnetization with the temperature we obtained only one Curie temperatures (Fig.3). It means that the contribution of the foreign phase to the magnetization is very small. The T_C and the maximum molar magnetization magnitude, p_{max}, (Tabs.3 and 4) decrease as the Co content increases.

The LHSCMO samples show a wide transition from ferromagnetic state at low temperature (Fig. 3) to paramagnetic state above the Curie temperature, T_C. This behaviour can be interpreted by the reduction of optimal Mn^{3+} amount, the decrease of the Mn-O_{eq}-Mn bond angles and Mn-O_{eq} bond lengths (Tab. 2) and the appearance of the cluster-glass state due to larger ionic radii of Co ions and a smaller tolerance factor, respectively, which may produce a decrease in the ferromagnetic double exchange interaction.

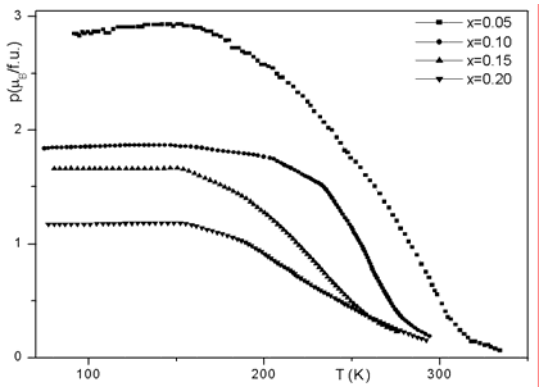

Fig. 3 Variation of molar magnetization (p) with temperature (T) and Co concentration (x)

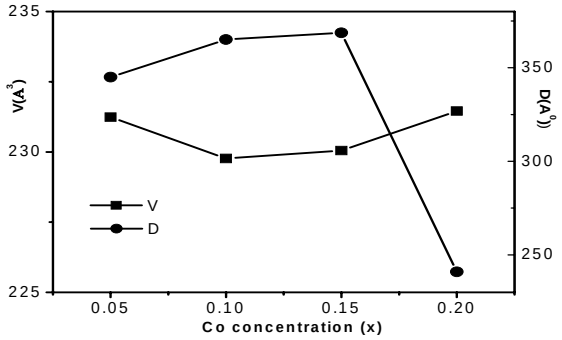

Fig. 4. Variation of unit-cell volume (V) and average size of the coherent blocks (D) for LHSCMO.

In addition, we can supposed that $Co^{2+/3+}$ ions with not participate in the double exchange interaction and electron hopping from Mn^{3+} ($t_{2g}^3 e_g^1$) to Co cations is energetically forbidden [1]. The broadening of FM-PM transition and decrease of T_C and p_{max} can be attributed to the small average size of the coherent blocks (Fig 1) and the higher grain boundary contribution arising from the weaker magnetic interaction near the grain boundary compared to the intra-grain contribution [15].

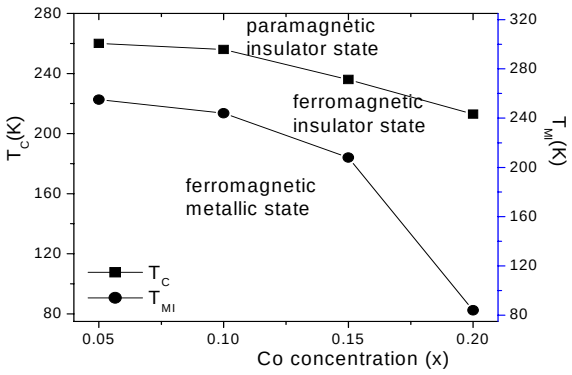

Fig. 5. Curie temperature and metal-insulator transition temperature dependence to the Co content for $La_{0.54}Ho_{0.11}Sr_{0.35}CoxMn_{1-x}O_3$ manganites.

Table 3 Variation of observed and calculated molar magnetization ($p_{max,\,obs}$ and p_{calc}) and bandwidth (w) for the LHSCMO manganites.

x	$p_{max,\,obs}$ (μ_B/f.u.)	p_{calc} (μ_B/f.u.)	w*	
			w_{ap}	w_{eq}
0.05	2.94	3.45	0.0952	0.0937
0.10	1.87	3.25	0.0954	0.0940
0.15	1.66	3.05	0.0938	0.0949
0.20	1.18	2.85	0.0928	0.0940

* calculated with the formula [14]:

$$w \propto \frac{\cos\left[\frac{1}{2}(\pi - \langle Mn-O-Mn \rangle)\right]}{d_{Mn-O}^{3.5}}$$

Table 4 Variation of observed and calculated molar magnetization ($p_{max,\,obs}$ and p_{calc}), bandwidth (w), calculated and observed average radii of B sites ($<r_{B,\,calc}>$, $<r_{B,\,obs}>$) Curie and transition temperatures (T_C, T_{MI}) for the LHSCMO manganites.

x	$<r_{B,\,calc}>$ (Å)	$<r_{B,\,obs}>$ (Å)	T_C (K)	T_{MI} (K)
0.05	0.5998	0.5302	260	236
0.10	0.5948	0.5292	256	215
0.15	0.5897	0.5382	236	184
0.20	0.5848	0.5448	213	84

The LHSCMO manganites behave different as metals at low temperatures and are characterized by a transition temperature from metal to the insulator-like behaviour (Fig. 6).

The temperatures corresponding to the resistance maxima decrease from 260 K (x=0.05) to 84 K (x=0.20) (Figs. 5 and 6). The observed values of the resistance for the LHSCMO manganites are due to the transport into the crystallites "core" (intrinsic magnetoresistance, supposing the absence of the defaults in the crystallite "core") and through the boundary layers of the crystallites (extrinsic magnetoresistance).

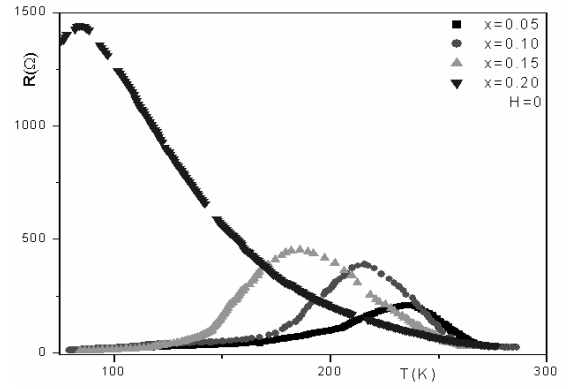

a)

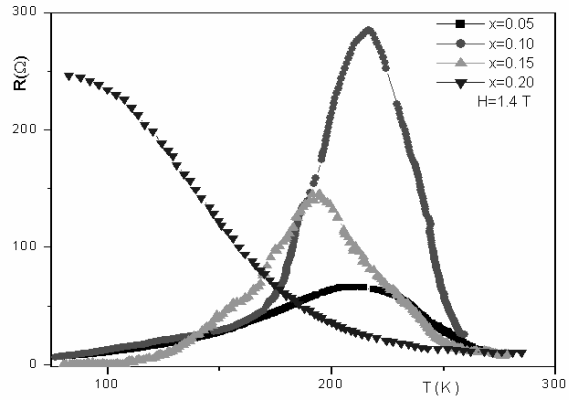

b)

Fig. 6. Variation of resistance with temperature (T) and Co concentration in the LHSMCO manganites (a- H=0; b) – H=1.4 T).

We have observed a magnetoresistive effect for all LHSCMO manganites (Figs. 5 and 6). Measurements of resistance at high temperature indicated that an enhancement of magnetoresistance appear near room temperature, similar to those observed in the substitution of Mn by Cr [16]. The variation of the magnetoresistance with the temperature indicated as possible the presence of two components: an extrinsic component, due to the transport of the carriers through the boundary layers, and an intrinsic component due to the transport of the carriers through the crystallite "core". In the investigated range of temperatures we observe broad maxima due to the boundary layers or to a region with high defaults concentration.

On other hand, the magnetoresistance temperature maxima are very large and their temperatures are far from the Curie temperature (Fig.6), 12) being due to the microdistortions and average size of crystallites (Fig1.).

4. Conclusions

A series of $La_{0.54}Ho_{0.11}Sr_{0.35}Co_xMn_{1-x}O_3$ manganites was obtained by ceramic method. All synthesized compounds have orthorhombic Pbnm structure. The specific magnetization is due only to the Zener type interactions between Mn cations. The substitution of Mn with Co led to a decrease of the specific magnetization and Curie temperature. The extrinsic magnetoresistance predominate in the $La_{0.54}Ho_{0.11}Sr_{0.35}Mn_{1-x}Co_xO_3$ synthesized manganites. Substitution of Mn with Co led to a decrease of the transition temperature.

References

[1] J. Hu, H.Qin, J. Chen, R. K. Zheng, J. Appl. Phys. **91**, 8912 (2002)
[2] D. Grossin, J.G. Noudem, Solid State Sciences **6**, 939 (2004).
[3] S. Cao, B. Kang, X.Wang, J. Zhang, G. Cao, L. Yu, C. Jing, Sol. St. Com. **134**, 265 (2005).
[4] X. Luo, W. Xing, Z. Li, G. Wu, X. Chen, Phys. Rev. **B 75**, 054413 (2007).
[5] S. Hebert, V. Pralog, D. Pelloquin, A. Maignan, J. Magn. Magn. Mater. **316**, 394 (2007).
[6] H. Y. Hwang, S. W. Cheong, N. P. Ong, B. Batlogg, Phys. Rev. Lett. **77,** 2041 (1996).
[7] C. Zener, Phys. Rev. **82,** 403 (1951).
[8] A. Gupta, J.Z. Sun, J. Magn. Magn. Mater. **200,** 24 (1999).
[9] S. P. Issac, N. D, Mathur, J. E. Evetts, M. G. Blamire, Appl. Phys. Lett. **72**, 2038 (1998).
[10] S. Grenier, J. P. Hill, V. Kiryukhin, W. Ku, Y.-J. Kim, K. J. Thomas, S-W. Cheong, Y. Tokura, Y. Tomioka, D. Casa, T. Gog, Phys. Rev. Lett. **94**, 047203 (2005)
[11] N. N. Loshkareva, E. A. Gan'shina, B. I. Belevtsev, Y. P. Sukhorakov, E. V. Mostovshchikova, A. N. Vinogradov, V. B. Krasovitsky, I. N. Chakanova, Phys. Rev. **B 68**, 024413 (2003)
[12] Y. Tokura and Y. Tomioka, J. Magn. Magn. Mater., **200**, 1 (1999).
[13] N. Cornei, C. Mita, M. L. Craus, Bull. Trans. Univ. Brasov **I,** 363 (2007).
[14] G. Papavassiliou, M. Fardis, M. Belesi, M. Pissas, I. Panagiotopoulos, G. Kallias, D. Niarchos, C. Dimitropoulos, J. Dolinsek, Phys.Rev. **59**, 6390 (1999)
[15] A. Dutta, N. Gayathri, R. Ranganathan, Phys. Rev. **B 68**, 54432 (2003).
[16] J. Hu, H. Qin, J. Chen, Sol. State Com. **124,** 437 (2002).

*Corresponding author: craus@phys-iasi.ro